National Geodetic Survey Positioning America for the Future geodesy.noaa.gov

NOAA Technical Report NOS NGS 75

Improvement of the GRAV-D Processing

Martin Willberg
Kevin Ahlgren
Philipp Zingerle
Roland Pail

Silver Spring, MD
January 2021

Contents

1 Introduction ... 1
2 Overview of airborne data ... 2
3 Gaussian low-pass filtering in the GRAV-D processing ... 4
3.1 Current GRAV-D implementation ... 4
3.2 Low-pass filter applied to gravity disturbances ... 6
4 Removed gravity observations ... 8
5 Offset and cross-over analysis ... 11
5.1 Offset from absolute gravity observations ... 11
5.2 Offset from a GGM ... 11
5.3 Offset from cross-over adjustment ... 11
5.4 Evaluation from cross-over adjustment ... 13
5.5 Discussion ... 14
6 Conclusion and outlook ... 15

Abstract

Airborne gravimetry from the Gravity for the Redefinition of the American Vertical Datum (GRAV-D) project is available for download in its current 'beta2' version. This report presents three main aspects where the processing of this GRAV-D data could be improved and evaluates them in block MS05 covering parts of Colorado and New Mexico. First, the application of the Gaussian low-pass filter should use gravity disturbances instead of absolute gravity values. This removes high-frequency noise of up to ±5 mGal from the airborne gravity observations, whereby the root mean square (RMS) of the improvement is 0.5 mGal in MS05. Second, the official GRAV-D data includes 11 observation gaps in MS05, but only one of these gaps is a clear outlier. Since data gaps will harm all applications of GRAV-D data, this report supports a less restrictive data removal and reinserts the 10 remaining gaps to the reprocessing (in order to prevent gaps in final product). Third, an analysis of individual flight line biases gives a significant improvement when flight line offsets are, for example, estimated in a cross-over analysis instead of the attachment to the absolute tie that is currently used. The analysis in this report indicates that applied airborne gravity corrections are responsible for systematic effects in the current GRAV-D solution. Since the cross-over analysis in this report is able to remove these systematic effects to a large extent, it provides a significant improvement toward the official GRAV-D solution. Additionally, the cross-over analysis for crossing flight lines allows a classification of the observation precision in GRAV-D. After implementing the three improvements of this report, the RMS of the observations is 1.3 mGal, while it was previously calculated as 2.3 mGal in MS05 (GRAV-D Team, 2018a). Accordingly, the adaptations in this study provide a significant improvement of up to 43%, which should be implemented in the near future and could benefit the definition of the new vertical datum as well as other applications.

Keywords GRAV-D · Airborne gravimetry · Low-pass filter · Data processing

1 Introduction

Gravity for the Redefinition of the American Vertical Datum (GRAV-D) is a multi-year project within NOAA's National Geodetic Survey (NGS) to measure airborne gravity across the entire United States and its territories (NGS, 2007). The primary outcome of this project is that it will provide the basis for a new vertical datum to be used for defining the nation's heights. This vertical datum, the North American-Pacific Geopotential Datum of 2022, will be based on a gravimetric geoid model and accessed through Global Navigation Satellite Systems (GNSS). As of January 2021, GRAV-D has already collected data over approximately 84% of the entire United States. The gravity data is collected along equally spaced flight lines with consistent flight characteristics (altitude, aircraft speed, sampling interval, etc.). The GRAV-D surveys are provided in data blocks that cover specific geographic regions of the United States. This report is completely focused on the MS05 block, which is approximately 650 km by 450 km and covers southern Colorado and northern New Mexico. This block is chosen for a number of reasons — the NGS has surveyed a high accuracy validation line in this region to serve as ground truth for geoid and gravity investigations (van Westrum et al., 2021). Additionally, the International Association of Geodesy (IAG)

Joint Working Group 2.2.2 called ‘the 1 cm geoid experiment’ (2017–2019) has published a number of geoid comparisons over this region (overview in Wang et al., in review). Furthermore, it is a region of rugged mountainous terrain, which provides a unique and difficult challenge for gravity and geoid modeling. While the analysis presented is specific to this block, the techniques and methods can be implemented and expanded to other areas.

This report is focused on three areas of concern within the current GRAV-D data processing: low-pass filtering of the raw gravity data, removal of gravity observations that don’t match a predetermined global geopotential model (GGM), and gravity offsets and trends between survey lines.

First, low-pass filtering is commonly applied in airborne gravity processing as the gravity data is dom-inated by high-frequency noise due to aircraft motion. However, in the current GRAV-D processing, the applied low-pass filter leaves significant high-frequency noise from aircraft motion that could be improved by a different filter application.

Secondly, there will always be individual situations where aircraft motion will cause the gravity ob-servations to be unrecoverable. In these situations, it is critical to remove the data thought to be in error. The current GRAV-D processing currently handles this identification and removal of data error through a combination of off-level correction and misfit to a GGM. This is performed on a case-by-case basis without a specific statistical threshold and subject to analyst bias. In the MS05 data block, almost all of the sections of data that are removedare likely to have been done so erroneously and could be reinserted to the final product.

Finally, the existence of offsets and trends in airborne surveys is not uncommon and can be caused by a number of different factors within the data collection and processing. The offset determination from a cross-over analysis by parameter estimation allows the calculation of individual flight line biases and the calculation of corresponding observation accuracies. However, the publicly available GRAV-D data does not account for any offset nor trend in the data lines. Within NGS, a gravity data offset is estimated and removed line-by-line prior to use for geoid modeling.

The report is structured as follows: In Section 2 we introduce the different data sets and different processing stages of GRAV-D that are used for this study. The Sections 3 to 5 separately handle three different aspects of the GRAV-D processing, which all improve the overall GRAV-D data quality and are described in this report. Section 3 addresses the Gaussian low-pass filter and explains the impact when filtering is applied to gravity disturbances instead of absolute gravity values. Next, Section 4 proposes and justifies an alternative method to detect (and remove) suspicious portions of the gravity observations, which result in significantly less data gaps in the GRAV-D product. Furthermore, the calculation of individual flight line biases is discussed in Section 5, which gives available options in airborne gravimetry and evaluates them based on their statistics. Finally, Section 6 draws conclusions from the report and gives an outlook for the GRAV-D processing in the future.

2 Overview of airborne data

This section describes which airborne gravimetry data are handled within this report and is intended to give an overview of the corresponding data sets. In general, we distinguish between original data (O1-O3), which were available before this study and the different versions of newly reprocessed data (R1-R3), which are created from the modifications proposed in this report. Furthermore, the two data sets (M1-M2) are synthesized from GGMs and are included for comparisons, validation and gravity reduction. Summarizing, the following data are handled:

1) O1 - Corrected raw observations:
   The available raw gravity observations include common corrections (e.g., aircraft motion, meter off-level error, and instrumental drift), which are described in *GRAV-D Team* (2017) and *Zhong et*

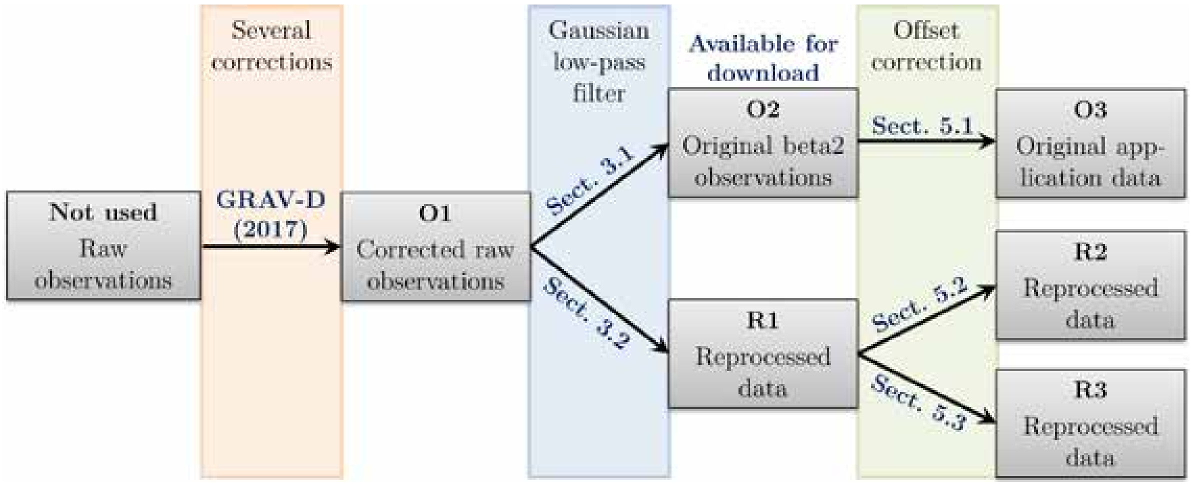

Fig. 1 Overview of data processing: original data (O1-O3) was available before this report, while the reprocessed data (R1-R3) results from improvements within this report. All arrows mark different processing steps, which are described in detail in the corresponding chapter.

al. (2015), but do not include a low-pass filter or an offset correction. The measurement frequency depends on the used instrument and is either 1 Hz or 20 Hz.

2) O2 — Original **beta2** observations:
The official, current version of the GRAV-D data is called "beta2" and is freely available for download. This report uses only the GRAV-D data of block MS05, which can be accessed on the corresponding website (GRAV-D Team, 2018b). Detailed explanations about the processing method in general can be found in GRAV-D Team (2017), while details about the instrumentation, the flight lines and the data quality of block MS05 are documented in GRAV-D Team (2018a). Beta2 data are calculated by applying a low-pass filter to the full-field gravity observations of O1 and include no offset correction. The measurement frequency depends on the gravity instrument used and is either 1 Hz or 20 Hz, but it is uniformly sampled to 1 Hz for comparisons in this report.
3) O3 — Original application data:
The original data set that is most beneficial for applications. It was produced from O2 in the context of the IAG working group "the 1 cm geoid experiment" (Wang et al., in review) and includes some useful modifications. The individual line bias is corrected by the Ref17A model (NGS, 2020) and the data are uniformly sampled to 1 Hz.
4) R1 — Reprocessed data without offset correction:
This data set is derived from the corrected raw observations (O1) by applying a Gaussian low-pass filter to the gravity disturbances and restoring the normal gravity afterwards. R1 realizes the modifications that are described in the Sections 3 and 4, but does not include an offset correction. The uniform frequency is 1 Hz.
5) R2 — Reprocessed data with offset correction from XGM2019e:
The data set R2 is calculated by including an offset correction from XGM2019e to R1. The calculation is described in Section 5.2.
6) R3 — Reprocessed data with offset correction from cross-over analysis:
The data set R3 is created by applying a cross-over analysis to correct individual flight line biases, whereby details are explained in Sect. 5.3.
7) M1 — Model observations from XGM2019e (Zingerle et al., 2020):
XGM2019e is the combination of a GGM and a topographic gravity field model. It is synthesized at 3D point level up to d/o 5540 and used for data reduction of airborne gravity measurements. As of October 2020, XGM2019e is the only high-resolution GGM that includes the newest satellite-only model (GOCO06S, Kvas et al. 2019) and furthermore the GGM with the highest spherical harmonic (SH) degree.

8) M2 - Model observations from EGM2008 (*Pavlis et al.*, 2012):
EGM2008 is used for comparisons in Section 4 and synthesized at 3D point level up to d/o 2190. It is the best-known high-resolution GGM and is furthermore used for the determination of observation gaps in the original data (O2 and O3, see Section 4).

3 Gaussian low-pass filtering in the GRAV-D processing

In the following, we describe the main differences between the original data sets (O1-O3) and the newly reprocessed versions (R1-R3). The corrected raw gravity observations (O1) in MS05 are superimposed by high-frequency noise, which results from the measurement in motion and is a common effect in airborne gravimetry (*Schwarz & Wei*, 1995; *Childers et al.*, 1999; *Olesen*, 2003). As a result of this noise, the gravity signal is not directly visible in the raw gravity observations, even after applying the corrections for aircraft motion, meter off-level error, and instrumental drift. Details about the corrections applied in the GRAV-D data are provided in *GRAV-D Team* (2017) and *Zhong et al.* (2015). After applying these corrections, the gravity signal can be extracted by applying a low-pass filter. For more details about the general approach of reducing noise in platform-stabilized airborne gravimetry we refer to *Childers et al.* (1999).

3.1 Current GRAV-D implementation

In the GRAV-D project a time-domain Gaussian filter is applied three times to the full-field gravity observations (*GRAV-D Team*, 2017, chapter 2.2; *GRAV-D Team*, 2018a, chapter 3.1). The filtering procedure is implemented using a Gaussian window where the weighting coefficients of the measurements n are computed based on

$$w(n) = \exp(-\frac{1}{2}\left(\alpha \frac{n}{(L-1)/2}\right)^2) \quad (1)$$

where $-(L-1)/2 \leq n \leq (L-1)/2$. L is the window length and α a width factor, which is (for a constant frequency) inversely proportional to the standard deviation σ of the Gaussian probability density function. Parameters used during the filter process are defined as follows:

Table 1 Gaussian filter parameters used for the original data processing (O2 and O3).

Frequency	L	α	σ
1 Hz	121	2.5	24
20 Hz	2401	2.5	480

Correspondingly, the full gravity signal and the observation noise are both filtered by the Gaussian low-pass filter, which is originally only intended for the observation noise. We consider this filter approach as disadvantageous, as gravity changes in the measurements result not only from signal variations, but also from changes in the height of the aircraft. Accordingly, the Gaussian low-pass filter implemented in *GRAV-D Team* (2018a,b) will smooth or remove gravity changes from height variations, which results in high-frequency noise in the gravity disturbances

$$\delta g = g - \gamma \quad (2)$$

Fig. 2 illustrates for the gravity disturbances of a 100 km segment of FL506, where the original processing O2 in blue shows unrealistic high frequencies compared to the new processing R1 (orange). In the new processing (e.g., R1), the Gaussian filter is used for gravity disturbances δg instead of full-field gravity values g and therefore independent (to the first order) of the flight elevation (*Forsberg et al.*, 2000), as is explained in detail in Section 3.2.

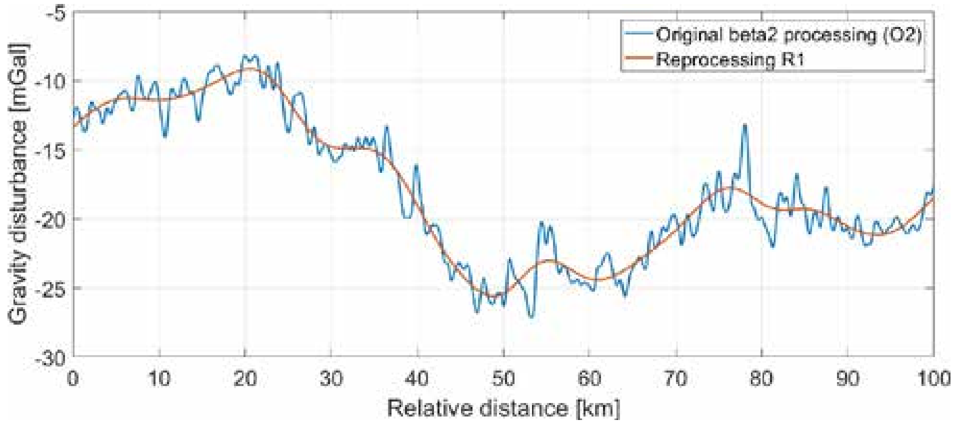

Fig. 2 Gravity disturbance comparison between the noisy original processing (O2, blue) and the reprocessed values (R1, orange) for a 100 km segment of flight line 506. This shows the improvement of the reprocessing strategy, as both solutions use an identical, but differently applied Gaussian low-pass filter.

The issue with the processing *GRAV-D Team* (2018a,b) is explained for the calculation of gravity disturbances δg in an error-free scenario. Therefore, we assume that the airborne gravity observations g and the normal gravity γ are identical and both able to describe the true gravity field along a 10 km part of flight line (FL) 203. The flight height of the selected flight segment is displayed in Fig. 3a, while Fig. 3b gives the corresponding normal gravity γ as well as the gravity observations g. Fig. 3c presents the resulting gravity disturbance δg, which is zero in the error-free case.

However, this changes as soon as we apply a Gaussian low-pass filter according to the specifications from the GRAV-D project. The filter does not affect the flight height (Fig. 4a) or the normal gravity γ, but only the gravity observations g (Fig. 4b). As a result, the gravity disturbances δg in Fig. 4c include absolute values of about 5 mGal, although gravity observations and normal gravity are still assumed as identical and error-free. We conclude that this effect is an error introduced by filtering full-field gravity observations, implicitly assuming a constant observation height. The resulting error in the gravity disturbances is highly correlated to the relative height of the aircraft (compare Fig. 4a and 4c), which changes due to winds, turbulences and flight control, therefore resulting in noise-like high-frequency effects for the gravity disturbance. In Fig. 4, for example, the frequency of the resulting error corresponds approximately to a SH degree 3000. The size of the error can be approximated by multiplying the vertical gravity gradient (0.3086 mGal/m) and the flight height difference to the local mean height. For the example in Fig. 4, the single-sided height change is approximately -15 m and results in a gravity disturbance error of about -5 mGal.

The preceding example highlights the problem of the current filter strategy, but the calculation of gravity disturbances is not the only case where it could be disadvantageous. Airborne gravity measurements in the current processing strategy depend significantly on the corresponding flight trajectory, which leads to the following problems:

1) Changes in the height of the aircraft (e.g., from winds) will significantly affect the quality of the gravity observations.
2) Full-field gravity variations from changes in the observation height will be smoothed and almost removed by the Gaussian low-pass filter (Fig. 4b). As a result, local minima in the flight height, for example, will inevitably result in an underestimation of the gravity observation at this point, as its observation is filtered (averaged) with smaller gravity values from higher-lying observations.
3) The processing strategy might even lead to a trend along a flight line segment, when there is a monotonic, but not constant change in the observation height (e.g., from a north-south trajectory). This trend would not only be visible in the gravity observations, but could also propagate to other derived gravity functionals, e.g., the geoid height N.

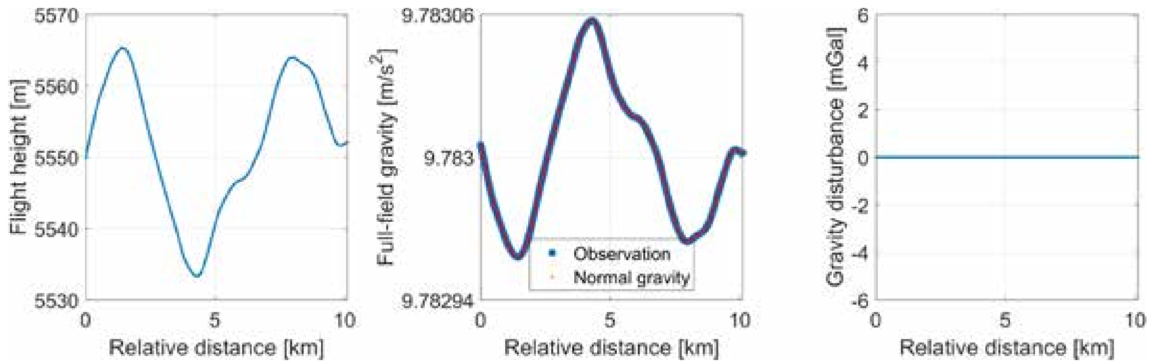

Fig. 3 Error-free and unfiltered observations along selected flight segment of FL 203. a) Flight height. b) Normal gravity and gravity observations. c) Resulting gravity disturbance.

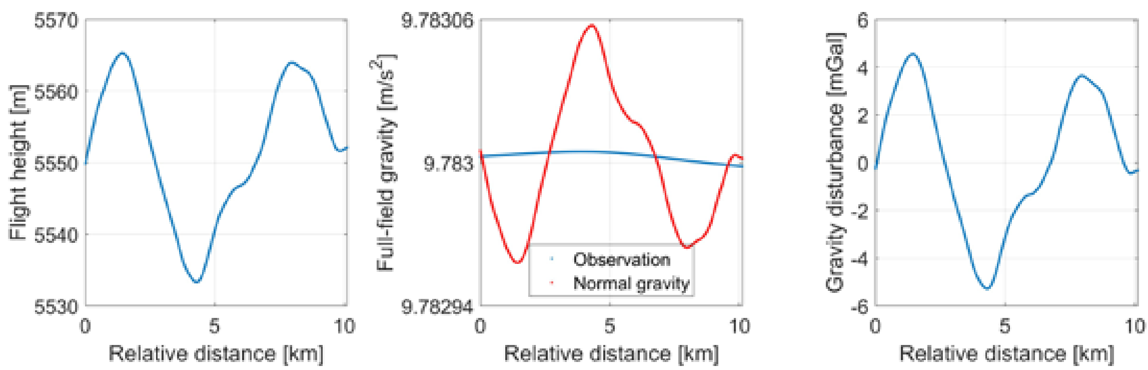

Fig. 4 Error-free, but filtered observations along selected flight segment of FL 203. a) Flight height. b) Normal gravity and gravity observations. c) Resulting gravity disturbance.

3.2 Low-pass filter applied to gravity disturbances

The described error, which is included by filtering gravity observations from different observation heights, can be removed (to first degree) when the Gaussian low-pass filter is applied to the gravity disturbances δg instead of the full-field gravity observations g. In this case, the gravity change from differences in the observation height is approximated by the normal gravity γ, and therefore eliminated to the first order in the gravity disturbance δg. After applying the low-pass filter to the gravity disturbances, the normal gravity is restored to the filtered gravity disturbances in order to result in the filtered, full-field gravity values g^{R1}

$$g^{R1} = A^G(g - \gamma) + \gamma \,, \tag{3}$$

or filtered gravity disturbances δg^{R1} respectively

$$\delta g^{R1} = A^G(g - \gamma) \,, \tag{4}$$

whereby A^G is the functional model for a Gaussian low-pass filter (with more details in *Willberg et al. 2020*). The values g^{R1} and δg^{R1} are referred to as R1 data, which is the reprocessed version without offset correction. δg^{R1} is presented in Fig. 6a and varies from approximately -40 to 120 mGal. We highlight at this point, that our goal is to evaluate differences from the change in the application of the filter. Accordingly, we apply a Gaussian low-pass filter in the same way as it is applied in the original processing (O2 and O3) instead of evaluating different low-pass filters or filter lengths in order to optimize the signal to noise ratio.

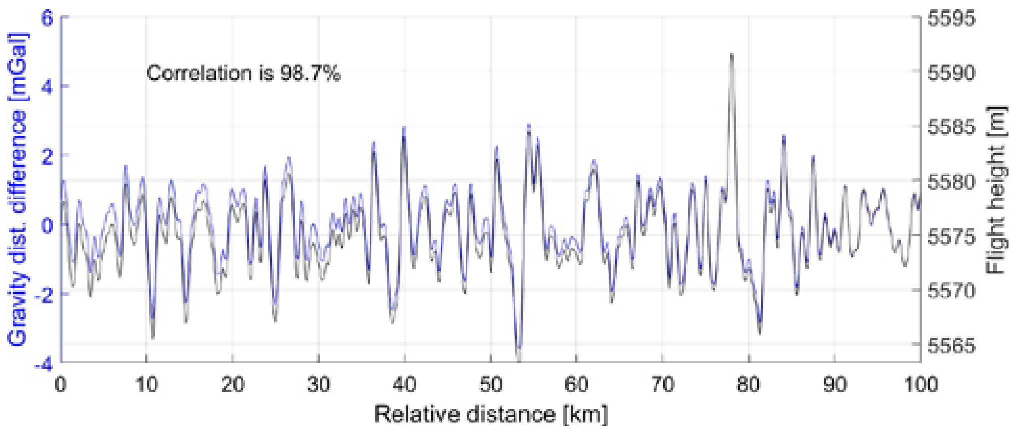

Fig. 5 The gravity disturbance difference between the original and the reprocessed GRAV-D data in blue (left axis) is correlated to the flight height in black (right axis). The very high correlation proves that the height changes of the aircraft are the reason for the processing differences. The gravity disturbance difference in blue equals the improvement of the reprocessed data.

Although, the additional cost of this improvement is minimal, it removes high-frequency artifacts from the observations, which is visible in Fig. 2, where the new processing (R1) is much smoother than the noisy original GRAV-D processing (O2). This difference results from height changes of the aircraft (see Fig. 4), which is also verified by Fig. 5. Fig. 5 presents the difference between the original (O2) and the new processing (R1) from Fig. 2 in the left axis (blue) together with the corresponding flight height in the right axis (black). The correlation of the two curves in the presented flight segment is 98.7%, which proves that the noise in the original processing results almost completely from the low-pass filter. The standard deviation of the presented difference (Fig. 5, blue) is 1.1 mGal, which constitutes the improvement of the new processing in this flight segment.

Fig. 6b shows the same comparison between the original processing (O2) and the reprocessed data (R1) for all flight lines of MS05. It confirms that the noise presented in Fig. 2 is included in all flightlines, but has different magnitudes. While most observation points have absolute differences below 0.7 mGal, a few flight lines show whole segments with values regularly exceeding ±3 mGal. The RMS of the improvement in Fig. 6b is 0.5 mGal, while the mean value is zero (since both solutions include no offset correction). The magnitude of the improvements is not distributed equally in MS05, but negatively correlated with the flight height (-20%). However, there is also a correlation between flight height and topography as well as flight height and the used gravity instrument (*GRAV-D Team*, 2018a). Accordingly, it is not possible to connect a single reason to the height movements of the aircraft, which are responsible for the differences in Fig. 6b.

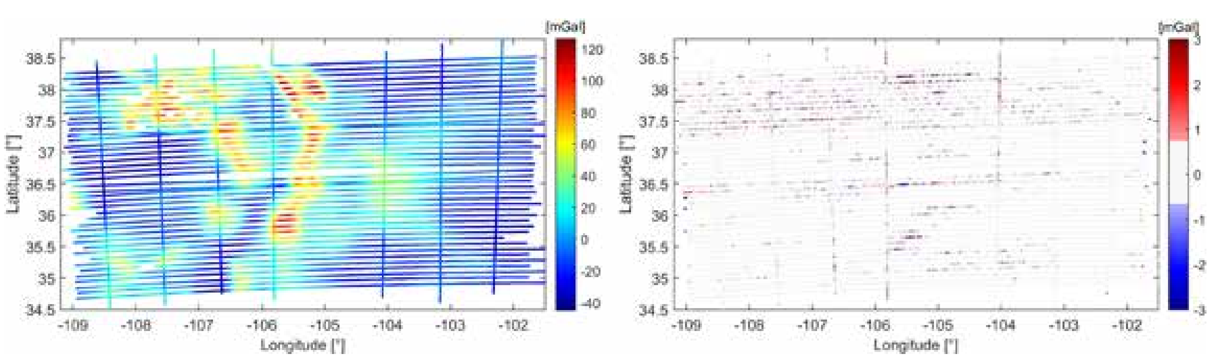

Fig. 6 Newly reprocessed R1 data are the result of applying a Gaussian low-pass filter to gravity disturbances in MS05 a) Gravity disturbance δg^{R1} b) Difference between the original 02 data and the newly reprocessed R1. Both solutions do not include any offset corrections.

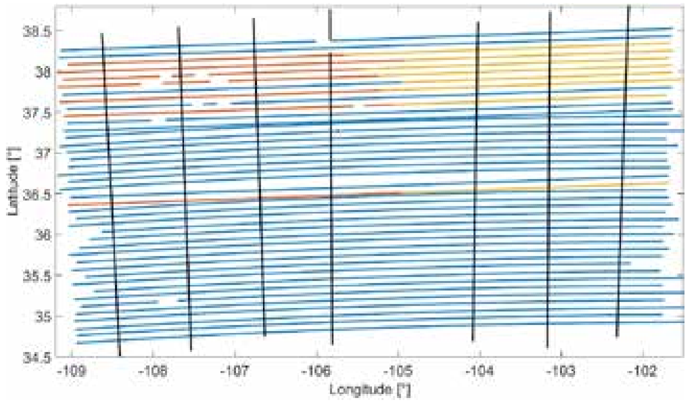

Fig. 7 Location of the airborne observations with the 11 gaps in the original processing. We differ cross-lines (black) and data-lines. The data-lines are further divided by long lines (blue) and short lines (red or yellow).

It should be noted that the two processing strategies (original vs. reprocessing) include different data trimming for the 'outside points.' Correspondingly, the differences that can be seen at the end of some flight lines are likely to be affected by the different data handling, as will be investigated by further studies. This is justified by the fact that different flight blocks of GRAV-D have significant overlaps, so that the last few kilometers of a flight line will have only insignificant importance to final gravity or geoid products.

In summary, the original processing strategy in O2 and O3 creates high-frequency noise, which depends on the height movements of the aircraft. This noise can be removed by applying the Gaussian low-pass filter to gravity disturbances (new processing) instead, which brings an average improvement of 0.5 mGal in MS05.

4 Removed gravity observations

Fig. 7 shows the location of data-lines (east-west direction) and cross-lines (black, north-south direction) of the original GRAV-D processing (O2,O3) in MS05 (*GRAV-D Team*, 2018a). In the figure, the east-west lines are additionally differentiated between long data-lines (blue) and short data-lines (red & yellow), since some of them actually originate from two different flights. It can be seen that several of the flight lines include (data) gaps, which are analyzed in the following.

In the original GRAV-D processing, only airborne observations taken while the aircraft is stable and on-line are considered valid for further use (these are presented in Fig. 7). Observations during take-off, transit, and landing are subject to many external motions and accelerations that make the gravity field too difficult to recover accurately. Practically, this requires the data to be trimmed to only certain sections of the flight. Additionally, there are certain portions of the flight where turbulence or other aircraft motion can degrade the gravity data collection. These occurrences are determined by looking at the off-level correction, operator field logs and comparisons with an a priori gravity field model (EGM2008). There is some degree of subjectivity to this process as no two data collection lines experi- ence the same circumstances. Portions of the flight that show a significant degradation or inconsisten- cies with the a priori model are removed and not used for geoid modeling or public release, therefore resulting in data gaps. While the GRAV-D block manuals (e.g., *GRAV-D Team* 2018a) identify where specific flight segments are removed, they give no concrete reason for the removal. As a result, the gravity measurements of MS05 include observation gaps at a total of 11 places in 8 different flight lines (Fig. 7). These observation gaps have a maximum length of 25 km with an average of approximately 18 km. Their location is mostly in areas with fast changing gravity signal and mountainous topography.

We consider the current criteria for outlier detection as overcautious, since the observation gaps could be a significant problem for further applications. However, the reprocessing gives realistic results for a majority of the original data gaps, which is shown in Fig. 8 and Tab. 2. Accordingly, we consider it generally beneficial to reinsert most data gaps to the final product. It should be noted that in Fig. 8 both the original processing O3 and the new processing R2 include a constant offset correction, which is explained in Sect. 5.

The different pictures in Fig. 8 show all data gaps of MS05 in detail and give different data sets for the corresponding flight segments. They include the original processing (O3) in black, which clearly presents the extent of the data gap. Additionally, the images include the newly reprocessed data (R2) in blue and the two gravity models XGM2019e (red) and EGM2008 (magenta). It can be seen that in all data gaps the reprocessed signal R2 differs significantly from EGM2008, which was one of the possible reasons to delete these segments in the original data. Tab. 2 confirms that XGM2019e fits generally much better to the gravity observations (black and blue) than EGM2008 and gives the corresponding RMS values. These RMS values are given for reduced gravity disturbances, which are calculated by subtracting synthesized gravity values (XGM2019e or EGM2008) from the corresponding observations. For simplicity, we name the reduced gravity values from XGM2019e $red.\,\delta g_i^{R2}$

$$red.\,\delta g_i^{R2} = \delta g_i^{R2} - \delta g_i(XGM2019e)\,, \tag{5}$$

which equals blue minus red curve in Fig. 8. Tab. 2 shows that RMS values of $red.\,\delta g_i^{R2}$ in the gaps are higher than in the remaining flight line, but generally lower than the corresponding reduced gravity disturbances from EGM2008.

Table 2 RMS values of the observation gaps that could be reinserted to the processing. FL 111 is missing, as Fig. 8 proves the corresponding observation gap to include unrealistic gravity values.

Flight line i	Units	101	109	110	136	305	306	504
RMS($red.\,\delta g_i^{R2}$) in gap(s)	mGal	4.1	6.0	9.7	7.7	5.1	6.3	5.9
RMS($red.\,\delta g_i^{R2}$) whole line	mGal	3.2	4.0	4.9	3.2	4.3	5.2	3.1
RMS($\delta g_i^{R2} - \delta g_i$(EGM2008)) gap(s)	mGal	11.0	7.4	13.5	9.1	11.1	10.3	4.9

We consider the following problems for using EGM2008 in the detection of observation gaps:

1) Segments where the a priori model (EGM2008) does not fit the observations, could result from insufficient data quality of the a priori model (e.g., resulting from old terrestrial gravity observations or missing GOCE information). This is particularly relevant for the presented data gaps, which all have high variations in the gravity disturbance along the flight segment.
2) GRAV-D is intended to improve available gravity data. Segments where the gravity data differs from EGM2008 could include these aimed improvements. However, these flight segments are deleted as precaution from errors.
3) Differences between the gravity observations and EGM2008 could result from the limited resolution of the GGM. This seems to be the case in FL101, where XGM2019e perfectly follows the reprocessed observations, but EGM2008 is not able to describe the high-frequency swing within the data gap. Although, the signal content of airborne observations (in MS05) is mostly below SH degree 2160, the very high-frequency signals (above this degree) from highly mountainous topography cannot be represented by EGM2008.
4) In case the reprocessed gravity disturbances (R2) are compared to the XGM2019e model, the absolute difference of 10 gaps (out of 11) is not necessarily worse than other flight segments with very high variation in the gravity signal.

We consider only one of the 11 observation gaps as an obvious observation error and prefer to include the remaining 10 gaps to the processing in the data block. The one observation gap (FL111) which is still considered defective in the reprocessed data has absolute, reduced gravity disturbances above 150 mGal, which is almost 10 times larger than all other observations.

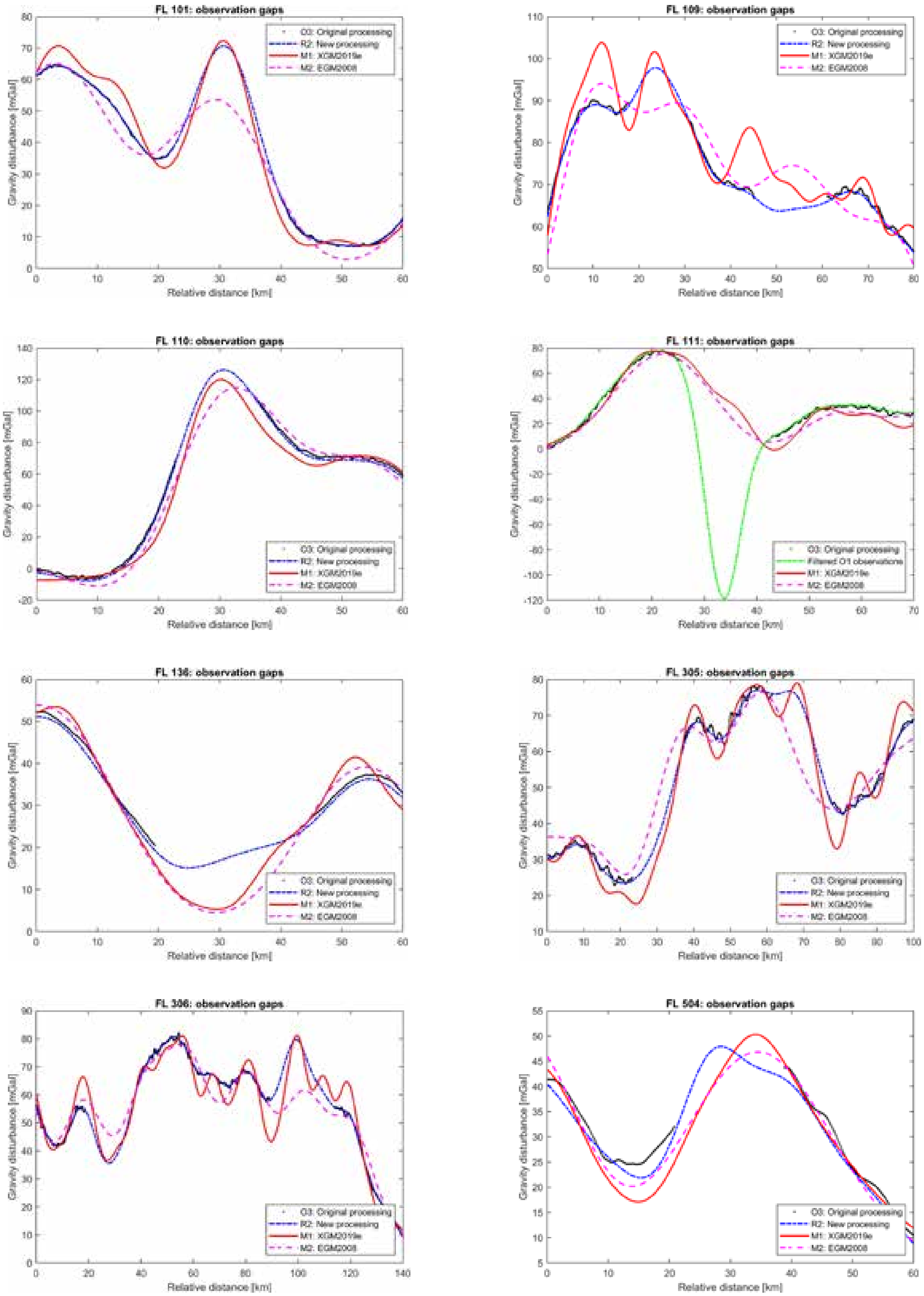

Fig. 8 Overview of the data gaps, which shows the original GRAV-D processing (black) and two synthesized GGM solutions XGM2019e and EGM2008 (red and magenta). 7 flight lines additionally include the new processing R2 (blue), while the gap in FL 111 is not reinserted to the reprocessing and shows only filtered O1 observations (green).

5 Offset and cross-over analysis

5.1 Offset from absolute gravity observations

In the original GRAV-D processing the raw observations are corrected for aircraft motion, meter off-level and drift *GRAV-D Team* (2017, chapter 2.2). Afterwards, the relative airborne observations are tied to an absolute gravity measurement at the airfield. The general approach of attaching GRAV-D observations to the absolute gravity measurement is explained in *GRAV-D Team* (2017, chapter 1.2.4), while the specific setup for the instruments of block MS05 is documented in *GRAV-D Team* (2018a, chapter 3.1). It should be noted that this gravity tie is also included in the O2 and R1 solution, which do not include further offset handling.

Although, this tie makes sense in theory, we observe an offset and sometimes a trend when we compare the original gravity observations (O2) to a GGM. As the long-wavelength part of a GGM is generally very accurate (e.g, *Gruber & Willberg* (2019)) and the majority of east-west flight lines in MS05 is approximately 650 km long, there should not be significant mean differences between the observations and the GGM. Therefore, this section evaluates if the gravity tie to an absolute gravity measurement at the airfield is prone to errors or whether the differences to the GGM result from data processing artifacts or random occurrences. Furthermore, it evaluates two alternatives to provide the relative airborne gravity observations with an absolute tie.

5.2 Offset from a GGM

The gravity observations could be tied to a GGM instead. In this case, the gravity observations of a single flight line are reduced with gravity values from a high-resolution GGM. Afterwards, the remaining, negative mean difference (Eq. 6) is added to all observations of that flight line (Eq. 7). The length of the flight lines in MS05 is within the resolution of the GOCE satellite mission, therefore generally well-determined in the long-wavelengths. However, it should be considered that this tie could be adverse affected by shorter wavelengths. If a satellite-only GGM is used for the offset determination, the omission error might affect the offset determination, as anomalies and topographic effects, for example, could introduce biases for specific flight line trajectories. While a high-resolution GGM would reduce this omission error significantly, local gravity effects are not necessarily correct in it either, so that the commission error might affect the determination of offsets. In general, the larger an area or the longer a flight line, the more stable is the determination of a corresponding offset, as a higher number of equally distributed measurements is more likely to be without bias from a GGM.

In the current setup, we apply XGM2019e to its maximum SH degree 5540 for the reduction of the airborne gravity disturbances. Thereby, we calculate the additive offset correction $\mu_{i,GGM}$ for a single flight line i from the corresponding reduced gravity disturbances ($red.\delta g_i^{R1}$, compare Eq. 5) using XGM2019e

$$\mu_{i,GGM} = -\text{mean}\,(\,red.\delta g_i\,). \tag{6}$$

Accordingly, the reprocessed airborne data

$$\delta g_i^{R2} = \delta g_i^{R1} + \mu_{i,GGM}\ , \tag{7}$$

is referred to as R2 solution. The original data O3 applies a similar correction, but utilizes the Ref17A model (*NGS*, 2020) instead of XGM2019e.

5.3 Offset from cross-over adjustment

Another method to calculate the flight line offsets is through parameter estimation. The so-called cross-over adjustment or cross-over (error) analysis is a common procedure in airborne gravimetry (*Becker* ,

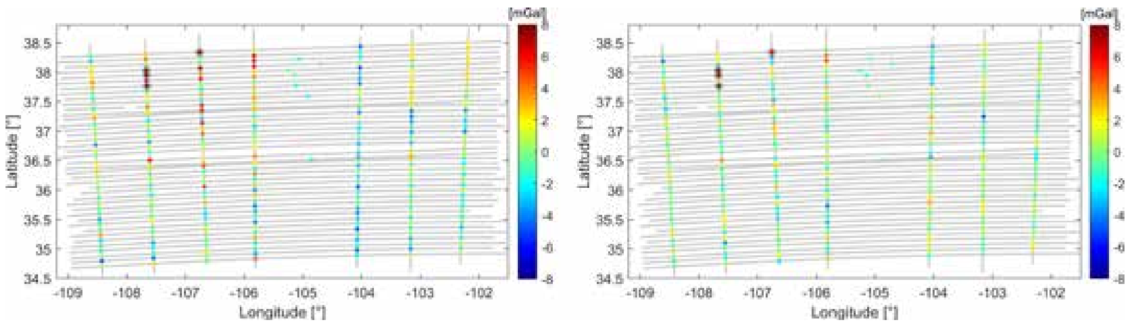

Fig. 9 Residuals at the 294 crossings before (a) and after (b) the cross-over analysis show the improvement from a bias correction. Panel a) uses the reprocessed data R1, while b) presents the residuals of R3 data. The flight lines are marked in gray and the four outliers are circled in black. The residuals are defined west-east minus north-south and western minus eastern flight line, respectively.

2016). This cross-over analysis calculates gravity differences at every flight line crossing and estimates one offset per flight line from these differences, which are called residuals. It should be noted that,in general, the corresponding two flight lines are not measured with the same flight height, so that gravity effects from height differences have to be considered in the calculation of residuals (*Forsberg et al.*, 2000). In this study, we approximate gravity differences from height variations by the XGM2019e model (M1). Accordingly, we compare the reduced gravity disturbances $_{red}.\delta g^{R1}$ (Eq. 5) of all flight lines at their crossing points for the cross-over analysis. For more details about the cross-over analysis it is referred to *Becker* (2016, chapter 7.1).

Altogether, the parameter estimation in MS05 includes 287 crossings between 49 data-lines and 7 cross-lines (compare Fig. 7). Additionally, 7 'crossings' can be added from overlapping data-lines at the location between the red and the yellow lines in Fig. 7. These additional crossings stabilize the offset estimation of the short lines significantly, as some of the short data-lines have only three intersections with the cross-lines. Both types of crossings are plotted with their residuals in Fig. 9, whereby we define the residuals as east-west minus north-south and western minus eastern flight line, respectively.

These residuals of the reprocessed data R1 (Fig. 9a) are used in the cross-over analysis to estimate the unknown flight line offsets $\mu_{i,est}$. Thereby, we flag residuals exceeding a 3-sigma criterion as outliers. In MS05, this results in four outliers among the 294 crossings when considering XGM2019e for the reduction of gravity data. Three out of these four outliers occur at crossings with one specific cross-line within only 40 km and they are clearly visible as dark red points in Fig. 9. At the moment, we can not give reasons for the high residuals along this specific flight segment, but we do not consider them to be gravity effects resulting from offsets between the flight lines. The crossing points of the outliers are not within one of the data gaps in the original data (cf. Sect. 4). Furthermore, it should be noted that the outliers are ignored for the estimation, but included in the RMS calculations.

Accordingly, the RMS of the residuals from the reprocessed data R1 in Fig. 9a is 2.72 mGal (Tab. 3). The resulting RMS error (RMSE, *Becker* 2016) is calculated by

$$RMSE = \frac{RMS}{\sqrt{2}}\,, \qquad (8)$$

and describes the typical scatter (or average observation accuracy) of a single flight line, which is 1.92 mGal for R1 data. The possibility to provide a quantitative validation of airborne gravity observations is a main advantage of the cross-over analysis and presented in detail in the next section.

The estimated flight line offsets $\mu_{i,est}$ range from approximately ± 3 mGal and are applied analog to Eq. 7 , so that the resulting gravity solution R3 is calculated by adding the estimated flight line offsets

Table 3 Overview of the RMS and RMSE values. Values in the last line are taken from *GRAV-D Team* (2018a), while all others are calculated from a cross-over analysis according to Sect. 5.3. The values in *GRAV-D Team* (2018a) are also used for the percentage improvement in terms of RMSE. The gravity tie is explained in the corresponding Sects. 5.1 (absolute), 5.2 (GGM) and 5.3 (cross-over).

Data set	Gravity tie	RMS [mGal]	RMSE [mGal]	Improvement of airborne observations
Reprocessed data R1	Absolute	2.72	1.92	17 %
Reprocessed data R2	GGM	2.03	1.44	38 %
Reprocessed data R3	Cross-over	1.87	1.32	43 %
Original data O2	Absolute	2.87	2.03	12 %
Original data O3	GGM	2.13	1.51	35 %
Original data O2 (accord. to *GRAV-D Team* 2018a)	Absolute	3.29	2.32	Reference

$\mu_{i,est}$ to the filtered gravity disturbances g^{R1} from Eq. 4

$$\delta g^{R3} = \delta g^{R1} + \mu_{i,est} \quad . \tag{9}$$

Lastly, the mean value of all reduced gravity disturbances (here <0.01 mGal) is set to zero, as the cross-over analysis itself can only estimate relative offsets between the flight lines.

5.4 Evaluation from cross-over adjustment

After applying the estimated offsets from the cross-over analysis, the resulting solution, identified as R3, is used to calculate the residuals at the crossing points again (Fig. 9b). The corresponding RMS value of the residuals in R3 is reduced to 1.87 mGal, while the RMSE of a single flight line goes down to 1.32 mGal. The RMSE can be interpreted as average observation accuracy and constitutes an improvement of 43% (for the reprocessed R3 data), when it is compared to the published values in *GRAV-D Team* (2018a). The RMS and RMSE values as well as the corresponding improvements of the observations are summarized in Tab. 3.

Using XGM2019e to correct flight line offsets (Sect. 5.2), the observation accuracy (RMSE) is 1.44 mGal, which is an improvement of 38%. The R1 data does not include any offset correction and is there- fore tied to absolute gravity observations similar to O2 (Sect. 5.1). Its RMSE calculation results in 1.92 mGal. The significant improvement of the RMSE values between the solution R1 (with absolute tie) and the solutions R2 and R3 (with offset correction from XGM2019e and cross-over analysis re- spectively) show a problem in the current tie of the GRAV-D observations.

In comparison to the reprocessed values, the cross-over analysis of the original airborne data (O2) in *GRAV-D Team* (2018a) gives a RMS of 3.29 mGal for the residuals and a corresponding RMSE of 2.32 mGal, which is used as a reference in Tab. 3. The following aspects are responsible for the 43% improvement (1 mGal in absolute values) in the observation accuracy between the documented values in *GRAV-D Team* (2018a) and the reprocessed version R3:

1) In the original data, gravity differences from different flight heights were approximated with the standard free-air correction, while the reprocessing calculates them from the XGM2019e model. As the height differences often reach more than 1000 m, the free-air correction might be too inaccurate to compensate for height differences at the crossing points.
2) The original airborne gravity data include a higher observation noise, as it applies the Gaussian low-pass filter to full-field gravity observations instead of gravity disturbances (Sect. 3).
3) Flight line offsets in R3 are estimated by the cross-over analysis, which will always decrease the RMS residuals (value is minimized in estimation).

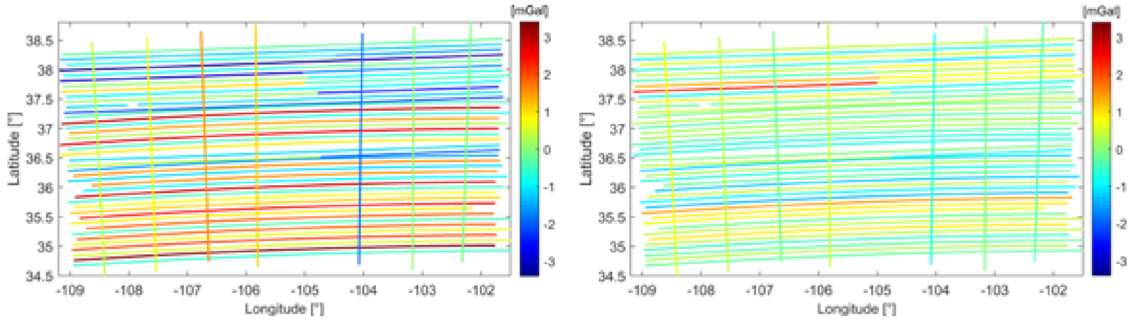

Fig. 10 Difference between the offset calculations described in the Sects. 5.1 to 5.3, where a) is cross-over analysis minus absolute tie (R3-R1) and b) is cross-over analysis minus offset from XGM2019e (R3-R2). The solutions R2 and R3 are fairly consistent, while they both differ significantly from R1.

4) Apart from the crossings between the so called data lines (east-west direction) and the cross-lines (north-south direction), we include 7 crossings from overlapping segments between two data lines. These 7 crossing are not included in the original calculations, but are also of minor importance in terms of the RMS value.
5) Residuals in *GRAV-D Team* (2018a) are calculated from the EGM2008 model, while the reprocessing uses the XGM2019e model, however this should not affect the RMS/RMSE calculation and is only included for the sake of completeness.

For a more consistent analysis of the improvement from the reprocessing, the original observations O2 should not be qualified by the values from *GRAV-D Team* (2018a), but by RMS/RMSE values calculated consistently with the steps in Sect. 5.3. In this case, the RMS of the O2 residuals is 2.87 mGal and the RMSE 1.97 mGal (Tab. 3). This gives an overall gravity observation improvement of up to 35% from the reprocessing, which is 0.7 mGal in absolute values.

5.5 Discussion

Summarizing the values from Tab. 3, we conclude the following:

1) Using an alternative to the absolute gravity tie is currently the most important processing improvement, so that the best solutions in terms of RMSE (R2, R3 and O3) include a bias correction based on a GGM (Sect. 5.2) or a cross-over analysis (Sect. 5.3).
2) Without the application of any reprocessing improvements, the more consistent calculation of RMSE values in this report already provides a 12% improvement in comparison to the calculation in *GRAV-D Team* (2018a).
3) Reprocessed GRAV-D values are improved by the application of the low-pass filter to gravity disturbances instead of full-field gravity values. However, the improvement in terms of RMSE is only about 0.1 mGal in average.

The quality of the reprocessed data sets R1 to R3 should not only evaluated by their statistics, but also by their actual differences. Fig. 10 gives the difference between R3 and R1 on the left and R3 minus R2 on the right. It can be seen that the solutions R2 and R3 are relatively consistent and their flight line offsets differ mainly within 1 mGal, while the difference in Fig. 10a exceeds 1 mGal for most of the flight lines. This supports the findings from Sect. 5.4 that in the current scenario, an offset determination from a GGM or cross-over analysis is better suited than the current gravity attachment to an absolute tie.

Nevertheless, there are also disadvantages: using the offset determination from a GGM, for example, will lose the independence of GRAV-D data from various GGMs. Furthermore, short flight lines are an issue for both offset determination methods. In MS05, long data lines are approximately 650 km long and have generally 7 crossings, while short flight lines have only 3 or 4 crossings and approximately half the length (Fig. 7). The longer a flight line is, the more accurate is the offset determination with a GGM (calculation of $\mu_{i,GGM}$). Or correspondingly, the more crossings a flight line has, the more accurate is the offset determination from the cross-over analysis (calculation of $\mu_{i,est}$). Accordingly, the short flight lines pose a significant problem in the determination of individual flight line offsets, which can only be solved when the flight lines are extended. In most cases an actual aircraft flight (from start to landing) includes two observed flight lines. Correspondingly, the offset calculation could theoretically be improved when these are combined for the offset determination. Respectively, this would lead to a longer flight line in Sect. 5.2 and a higher number of crossings in Sect. 5.3.

However, this idea cannot be realized at the moment, as there are some systematic effects either in the applied corrections (*GRAV-D Team*, 2017) or in the measurements of GRAV-D. We demonstrate this by comparing the reprocessed versions R1 (no offset correction) and R3 (offset correction from parameter estimation) with their difference given by $\mu_{i,est}$ (Eq. 9). When we consider only aircraft flights with at least one west to east and one east to west line, we can find the following systematic effects:

1) The offset correction $\mu_{i,est}$ is significantly higher for flights from east to west (0.89 mGal in average) than it is for flights from west to east (-0.84 mGal in average). This effect is clearly detectable from the parameter estimation, as all 13 flight combinations with only long data-lines have a higher offset correction $\mu_{i,est}$ for east to west flights than for west to east.
2) The offset correction $\mu_{i,est}$ is significantly higher for flights from Amarillo (Texas, 0.91 mGal in average) than it is for flights from Grand Junction (Colorado, -1.25 mGal in average).
3) Consequently, the highest offsets corrections $\mu_{i,est}$ are added to west to east flights flown from Amarillo (2.01 mGal in average), while the smallest are added to east to west flights from Grand Junction (-1.78 mGal in average).

These systematic effects are obviously correlated to the flight direction and we identify the applied corrections (*GRAV-D Team*, 2017) as most likely error source for that. Furthermore, there is a strong correlation to the airport that is used for the survey. However, this cannot be clearly connected to a single source: apart from the different airport, the three Texas surveys use a different aircraft and a different absolute gravity tie, but also different instruments and partly different years than the survey from Colorado. Furthermore, all short data-lines are flown within the Colorado survey and it should be mentioned that the Colorado flight lines are more often in highly mountainous areas. In our opinion, the systematic effects can only be solved completely by analyzing the uncorrected raw measurements or the applied corrections in detail, which should not be part of this study, but an aspect of further investigations. In case these systematic effects can be removed in the future, it will likely be beneficial to consider all flight lines between start and landing of the aircraft within a joint offset determination (regardless of the method that is used for the offset determination).

This might even enable the inclusion of a trend estimation and reduction in the future. In the current reprocessing, some of the flight lines show a small trend in comparison to XGM2019e. At the moment, it cannot be specified whether these trends result from the observations or other reasons (e.g., topographic reduction, random effects, flight trajectory). Combining all flight lines between start and landing of an aircraft would often result in observation lengths between 1200 and 1400 km, which might be sufficient to study possible trends in the gravity data.

6 Conclusion and outlook

The GRAV-D project is essential for the definition of the new North American vertical datum and with a lot of effort put in the acquisition of the airborne gravity data, their gain should be maximized by the processing. This report points out three aspects where the current `beta2` version of the GRAV-D processing (O2 in this report) could be improved.

First, applying the Gaussian low-pass filter to gravity disturbances instead of absolute gravity observations removes high-frequency noise effects from the observations. These effects result from small height changes of the aircraft during its flight and are completely removed in the reprocessed GRAV-D data. In MS05, the improvement of this adaption at flight height can amount up to 5 mGal with an average improvement of 0.5 mGal. The improvement is unequally distributed over the region, correlated to topography and flight height. However, adapting the application of the Gaussian low-pass filter will only have a small impact to the new vertical datum, as high-frequency noise effects have, in general, only minor consequences for the geoid.

Second, the detection of observation errors is likely overcautious in the original beta2 processing. At the moment, an increased difference between the GRAV-D observations and an a priori model is one of the possible reasons to remove observations from the processing. In our opinion, this may as easily result from the a priori GGM as it arises from suspicious airborne observations. As a result, specific flight segments, where the GRAV-D data might actually improve available GGMs could be accidentally removed from the processing. Furthermore, the data gaps will likely harm various applications of the GRAV-D data, so that we would recommend a more cautious removal of flight segments and trying to automate the procedure. In the example of this reprocessing, we result in only one instead of 11 observation gaps in MS05.

The third aspect concerns individual flight line offsets resulting from relative airborne gravimetry: the original GRAV-D processing attaches relative observations to an absolute gravity observation at the airfield. The evaluation and statistics from this report show that the attachment to a GGM or the estimation from a cross-over analysis provide more consistent results and yield much better statistics. While *GRAV-D Team* (2018a) calculates the observation accuracy of GRAV-D observations in MS05 as 2.32 mGal (RMSE), this study results in 1.32 mGal with an offset correction from the cross-over analysis. It should be mentioned that the improvement is not only from a better processing, but also from a more precise calculation of the observation accuracy. Accordingly, we consider an observation accuracy of 1.97 mGal for the original beta2 data (instead of the 2.32 mGal in *GRAV-D Team*, 2018a). In contrast to the high-frequency noise, the correction of the individual flight line offsets would have significant effects to the calculation of the geoid and the vertical datum. Further improvements and a more stable estimation of offsets might be possible in the future, when the overlap between different GRAV-D blocks is exploited to estimate their offsets together.

In considering any future updates, a high priority should be given to the analysis of systematic effects and errors that result in the flight line offsets in the official beta2 solution. The official GRAV-D data gives the gravity values for flight lines from east to west as too small, while they are too high for lines from west to east, approximately 0.8-0.9 mGal respectively in either direction. Furthermore, the gravity observations which are taken from Amarillo (Texas) are in average 2.2 mGal smaller than corresponding observations from Grand Junction in Colorado. Additional work needs to be done to completely isolate what is causing this line bias. It is unlikely that the bias is actually caused by errors in the absolute gravity tie at the airport, but it is possible that the absolute gravity tie is not consistent with the data processing corrections. Moreover, it is possible that these applied corrections are the cause of the bias problem. Work on this topic in ongoing (see *Childers & Kanney*, 2020) and shows promise for fixing this issue.

The current GRAV-D data product has always been released as a BETA version under the anticipation that a final (re)processing would occur prior to a 'FINAL' data release. While we do not comment on the timeline for this, the data processing and methodology changes laid out in this report would be quite straightforward to implement in a new data processing and provide a number of significant improvements. It is difficult to ascertain the degree to which improvements in the airborne data will impact the geoid — but at a bare minimum, the incorporation of a new GGM model resulting in the inclusion of omitted sections would provide necessary gravity information in previously unknown areas.

Acknowledgements

A significant part of the research performed for this report was conducted while the first author was a Visiting Scientist at NGS. The authors would like to thank Ryan Hardy, Steve Hilla, Dan Roman, and Derek van Westrum for reviewing and providing comments to this document.

References

Becker, D. (2016). "Advanced Calibration Methods for Strapdown Airborne Gravimetry," In: Schriftenreihe der Fachrichtung Geodäsie, TU Darmstadt, Darmstadt, Technische Universitat Darmstadt, ISBN 978-3-935631-40-2.

Childers, V.A., R.E. Bell, and J. Brozena (1999). "Airborne gravimetry: An investigation of filtering," *Geophysics*, 64(1): 61-69. https://doi.org/10.1190/1.1444530 .

Childers, V.A., and J. Kanney (2020). "The Airborne Gravity Off-Level Correction Revisited Using NGS GRAV-D Data." AGU meeting.

Damiani, T.M., M. Youngman, and J. Johnson eds., (2019). GRAV-D Team (2017) *GRAV-D General Airborne Gravity Data User Manual*. Version 2.1. Available Oct. 15, 2019.

Forsberg, R., A.V. Olesen, L. Bastos, A. Gidskehaug A, U. Meyer, and L. Timmen (2000). "Airborne geoid determination," *Earth Planets Space*, 52: 863-866. https://doi.org/10.1186/BF03352296 .

GRAV-D Team (2018b) Gravity for the Redefinition of the American Vertical Datum (GRAV-D) Project, Airborne Gravity Data; Block MS05. Available Oct. 15, 2019.

Gruber, T. and M. Willberg (2019). "Signal and error assessment of GOCE-based high resolution gravity field models," *Journal of Geodetic Science*, vol. 9, no. 1, pp. 71–86. https://doi.org/10.1515/jogs-2019-0008 .

Harlan, R.B. (1968). Eotvos corrections for airborne gravimetry, *J. Geophys. Res.*, 73(14), 4675– 4679, https://doi.org/10.1029/JB073i014p04675 .

Hirt, C. and M. Rexer (2015). "Earth2014: 1 arc-min shape, topography, bedrock and ice-sheet models — Available as gridded data and degree-10,800 spherical harmonics," *International Journal of Applied Earth Observation and Geoinformation* 39: 103–112. https://doi.org/10.1016/j.jag.2015.03.001

Kvas, A., T. Mayer-Gürr, S. Krauss, J.M. Brockmann, T. Schubert, W.S. Schuh, R. Pail, T. Gruber, A. Jäggi, and U. Meyer (2019). The satellite-only gravity field model GOCO06s. GFZ Data Services. https://doi.org/10.13140/RG.2.2.14101.99047 .

LaCoste, L.J. (1967). Measurement of gravity at sea and in the air. *Reviews of Geophysics*, 5(4): 477–526. https://doi.org/10.1029/RG005i004p00477 .

National Geodetic Survey (2007). The GRAV-D Project: Gravity for the Redefinition of the American Vertical Datum. Project plan, available at https://geodesy.noaa.gov/GRAV-D/pubs.shtml . Accessed: Nov. 10, 2020.

National Geodetic Survey (2019). Homepage at https://www.ngs.noaa.gov/GRAV-D/data_products.shtml . Accessed: Oct. 15, 2019.

National Geodetic Survey (2020). Experimental Geoid Models 2017. Homepage at https://beta.ngs.noaa.gov/GEOID/xGEOID17/ . Accessed: Oct. 26, 2020.

Olesen, A.V. (2003). *Improved airborne scalar gravimetry for regional gravity field mapping and geoid determination*. Dissertation, Faculty of Science, University of Copenhagen.

Pail, R., T. Fecher, D. Barnes D, J.F. Factor, S.A. Holmes, T. Gruber, and P. Zingerle (2018). "Short note: the experimental geopotential model XGM2016." *J Geod,* 92(4): 443-451. https://doi.org/10.1007/s00190-017-1070-6 .

Pavlis, N.K., S.A. Holmes, S.C. Kenyon, and J.K. Factor (2012). "The development and evaluation of the Earth Gravitational Model 2008 (EGM2008)." *J Geophys. Res.,* 117, B04406. https://doi.org/10.1029/2011JB008916 .

Rexer, M., C. Hirt, S. Claessens, and R. Tenzer (2016). "Layer-Based Modelling of the Earth's Gravitational Potential up to 10-km Scale in Spherical Harmonics in Spherical and Ellipsoidal Approximation." *Surv Geophys*, 37(6): 1035–1074. https://doi.org/10.1007/s10712-016-9382-2 .

Schwarz, K.P. and M. Wei (1995). "Some Unsolved Problems in Airborne Gravimetry." In: Sünkel H., Marson I. (eds) *Gravity and Geoid.* International Association of Geodesy Symposia, vol 113. Springer, Berlin, Heidelberg. https://doi.org/10.1007/978-3-642-79721-7_15 .

Swain, C.J. (1996). "Horizontal acceleration corrections in airborne gravimetry." *Geophysics*, 61(1): pp. 273–276. https://doi.org/10.1190/1.1443948 .

van Westrum, D., K. Ahlgren, C. Hirt, and S. Guillaume (2021). "A Geoid Slope Validation Survey (2017) in the Rugged Terrain of Colorado, USA." *J Geod* 95, 9. https://doi.org/10.1007/s00190-020-01463-8

Wang, Y.M., L. Sánchez, J. Ågren, J. Huang, R. Forsberg, H.A. Abd-Elmotaal, R. Barzaghi, T. Bašić, D. Carrion, S. Claessens, B. Erol, S. Erol, M. Filmer, V.N. Grigoriadis, M.S. Isik, T. Jiang, O. Koç, X. Li, K. Ahlgren, J. Krcmaric, Q. Liu, K. Matsuo, D.A. Natsiopoulos, P. Novák, R. Pail, M.Pitoňák, M. Schmidt, M. Varga, G.S. Vergos, M. Véronneau, M. Willberg, and P. Zingerle (SUBMITTED, 2020) Report on the 1-cm geoid experiment in Colorado. *J Geod*

Willberg, M., P. Zingerle P, and R. Pail (2020). "Integration of airborne gravimetry data filtering into residual least-squares collocation — example from the 1 cm geoid experiment." *J Geod* 94, 75. https://doi.org/10.1007/s00190-020-01396-2 020-01396-2 .

Youngman, M. and J. Johnson eds. (2019). GRAV-D Team (2018a) Block MS05 (Mountain South 05), GRAV-D Airborne Gravity Data User Manual. Version BETA#2. Available Oct. 15, 2019.

Zhong, D., and T.M. Damiani, S.A.M. Preaux, and R. Kingdon (2015). "Comparison of airborne gravity processing results by GravPRO and Newton software packages." *Geophysics*, 80(4): G107-G118. https://doi.org/10.1190/geo2014-0519.1 .

Zingerle, P., R. Pail, T. Gruber, and X. Oikonomidou (2020). "The combined global gravity field model XGM2019e." *J Geod* 94, 66 (2020). https://doi.org/10.1007/s00190-020-01398-0 .